Supporting Information

A new visible light excitable ICT-CHEF mediated fluorescence 'turn on' probe for the selective detection of Cd^{2+} in aqueous system with live-cell imaging

Shyamaprosad Goswami,*[a] Krishnendu Aich[a], Sangita Das[a], Chitrangada Das Mukhopadhyay[b], Deblina Sarkar[c] and Tapan Kumar Mondal[c]

[a] *Department of Chemistry, Indian Institute of Engineering Science and Technology, Shibpur, Howrah-711 103, India. Fax: +91 33 2668 2916; Tel: +91 33 2668 2961-3;*
E-mail: spgoswamical@yahoo.com

[b] *Department of Centre for Healthcare Science & Technology, Indian Institute of Engineering Science and Technology, Shibpur, Howrah-711 103, India*

[c] *Department of Chemistry, Jadavpur University, Jadavpur, Kolkata, India*

CONTENTS

1. ***Determination of detection limit……..***
2. ***Determination of association constant……***
3. ***Linear responsive curve of BPQ depending on Cd^{2+} concentration……..***
4. ***Job plot……..***
5. ***Competition Study……..***
6. ***Determination of Quantum yield……..***
7. ***pH study……..***
8. ***Computational study……..***
9. ***Live cell imaging……***
10. ***^{1}H NMR spectrum of BPQ……***
11. ***^{13} C NMR spectrum of BPQ……..***
12. ***Mass spectrum (HRMS) of BPQ ……..***
13. ***^{1}H NMR titration of BPQ with Cd^{2+}……..***
14. ***FT-IR spectra of BPQ and its Cd^{2+}complexes……..***
15. ***MS spectrum of Cd^{2+} complex of BPQ…….. ……....***
16. ***References……..***

1. **Determination of detection limit:**

From the concentration dependent graph (b) we can determine minimum 9.95×10^{-8} M concentration of Cd^{2+}, using 1μM of BPQ.

2.

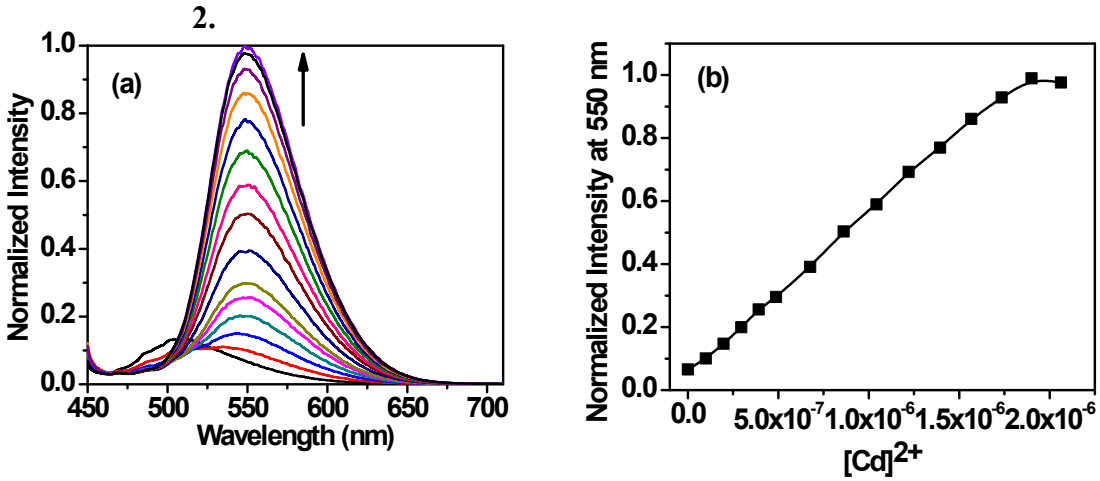

Figure S1: (a) Emission spectra of BPQ (1 μM) upon incremental addition of Cd^{2+} (0 to 2.0 μM) in CH_3CN/H_2O (2/3, v/v) solution. (b) Emission of BPQ at 550 nm depending on the concentration of Cd^{2+}. λ_{ex} = 430 nm.

2. **Determination of Association Constant (K_a):**

By UV-vis method:

Association constant was calculated according to the Benesi-Hildebrand equation. K_a was calculated following the equation stated below.

$$1/(A-A_o) = 1/\{K(A_{max}-A_o)\,[M^{x+}]^n\} + 1/[A_{max}-A_o]$$

Here A_o is the absorbance of receptor in the absence of guest, A is the absorbance recorded in the presence of added guest, A_{max} is absorbance in presence of added $[M^{x+}]_{max}$ and K_a is the association constant, where $[M^{X+}]$ is $[Cd^{2+}]$. The association constant (K_a) could be determined from the slope of the straight line of the plot of $1/(A-A_o)$ against $1/[Cd^{2+}]$ and is found to be 7.82×10^4 M^{-1}.

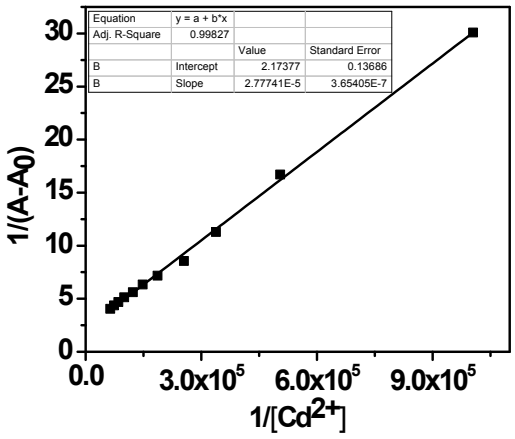

Figure S2: Benesi-Hildebrand plot from absorption titration data of receptor (10 μM) with Cd^{2+}.

By fluorescence method:

The binding constant value of Cd^{2+} with receptor has been determined from the emission intensity data following the modified Benesi–Hildebrand equation, $1/\Delta I = 1/\Delta I_{max} + (1/K_a[C])(1/\Delta I_{max})$. Here $\Delta I = I - I_{min}$ and $\Delta I_{max} = I_{max} - I_{min}$, where I_{min}, I, and I_{max} are the emission intensities of receptor considered in the absence of Cd^{2+}, at an intermediate Cd^{2+} concentration, and at a concentration of complete saturation where K is the binding constant and [C] is the Cd^{2+}concentration respectively. From the plot of $[1 / (I - I_{min})]$ against $[C]^{-1}$ for receptor, the value of K has been determined from the slope. The association constant (K_a) as determined by fluorescence titration method for the receptor with Cd^{2+} is found to be $1.55 \times 10^5\ M^{-1}$.

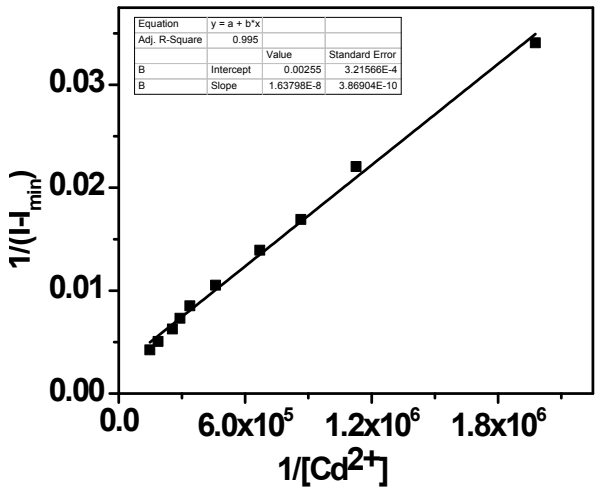

Figure S3: Benesi–Hildebrand plot from fluorescence titration data of receptor (10 μM) with Cd^{2+}.

3. Linear responsive curve of BPQ depending on Cd^{2+} concentration:

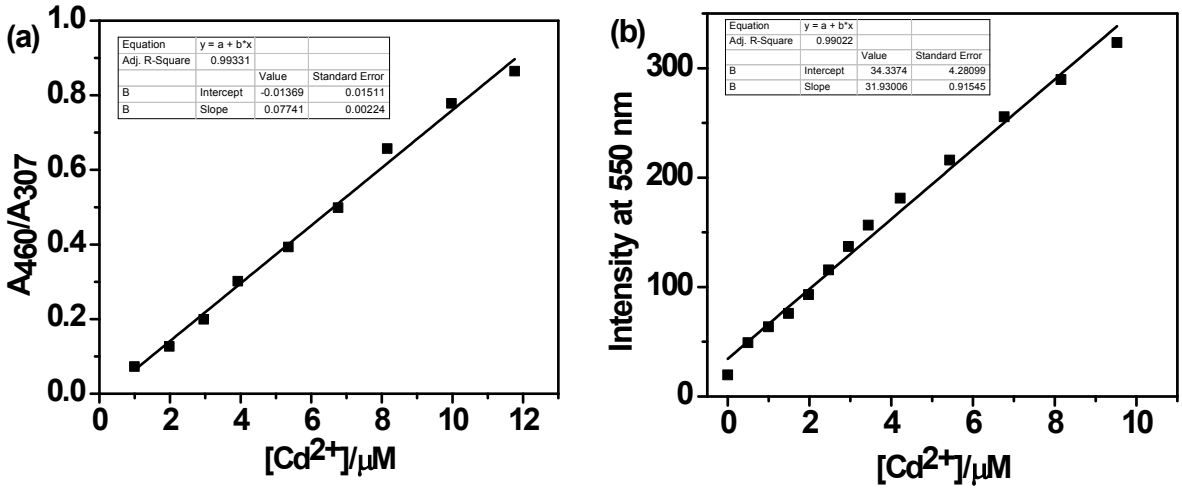

Figure S4: The linear response curve of (a) absorbance ratio (A_{460}/A_{307}) and (b) emission intensity at 550 nm of BPQ depending on the Cd^{2+} concentration.

4. General procedure for drawing Job's plot by fluorescence method:

Stock solution of same concentration of sensor and Cd^{2+} was prepared in the order of 10 μM in [CH_3CN/ H_2O, 2/3, v/v] (at 25 °C) at pH 7.3 in HEPES buffer. The emission spectrum in each case with different *host–guest* ratio but equal in volume was recorded. Job's plots were drawn by plotting $\Delta I.X_{host}$ *vs* X_{host} (ΔI = change of intensity of the emission spectrum at 550 nm during titration and X_{host} is the mole fraction of the host in each case, respectively).

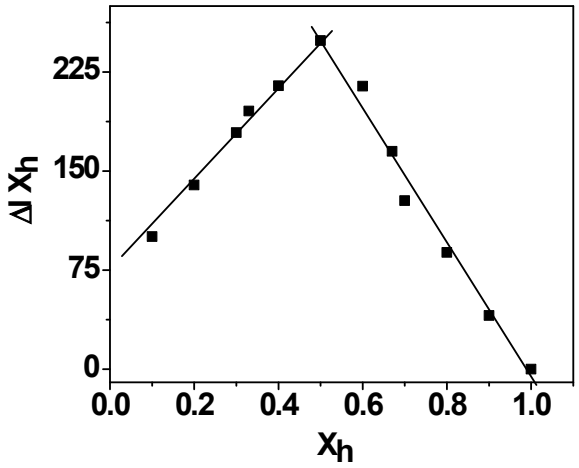

Figure S5: Job's plot diagram of receptor for Cd^{2+} (where X_h is the mole fraction of the host and ΔI indicates the change of emission intensity at 550 nm).

5. Competition study

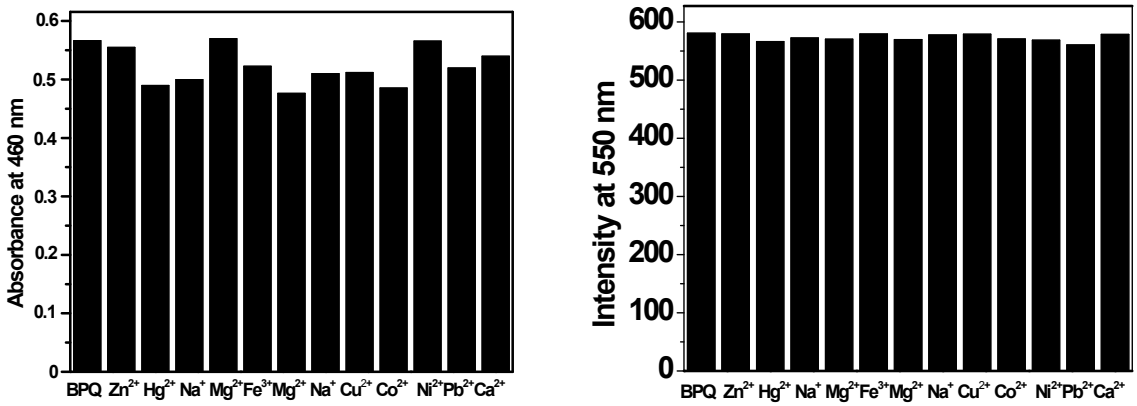

Figure S6: Competition study using (a) UV-vis and (b) Fluorescence method, after addition of different analytes (30 μM) in the solution of BPQ (10 μM) in presence of Cd^{2+} (20 μM).

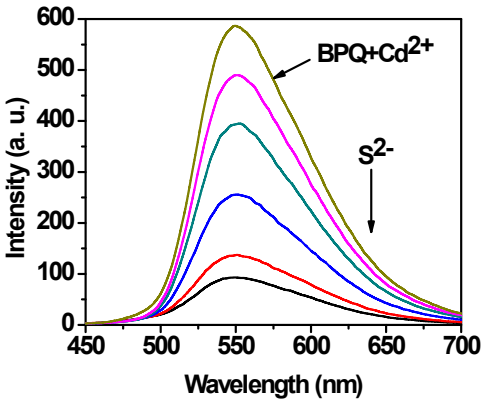

Figure S7: Fluorescence titration spectra of BPQ-Cd^{2+} (10 μM) upon increasing concentration of S^{2-} (0 to 10 equivalents). λ_{ex} = 430 nm.

6. Determination of fluorescence Quantum Yields (Φ) of BPQ and its complex with Cd^{2+} ion:

For measurement of the quantum yields of BPQ and its complex with Cd^{2+}, we recorded the absorbance of the compounds in methanol solution. The emission spectra were recorded using the maximal excitation wavelengths, and the integrated areas of the fluorescence-corrected spectra were measured. The quantum yields were then calculated by comparison comparison with fluorescein (Φs = 0.97 in basic ethanol) as reference using the following equation:

$$\Phi x = \Phi s \times \left(\frac{Ix}{Is}\right) \times \left(\frac{As}{Ax}\right) \times \left(\frac{nx}{ns}\right)^2$$

Where, x & s indicate the unknown and standard solution respectively, Φ is the quantum yield, *I* is the integrated area under the fluorescence spectra, *A* is the absorbance and *n* is the refractive index of the solvent.

We calculated the quantum yield of BPQ and BPQ-Cd^{2+} using the above equation and the value is 0.02 and 0.46 respectively.

7. pH dependent study:

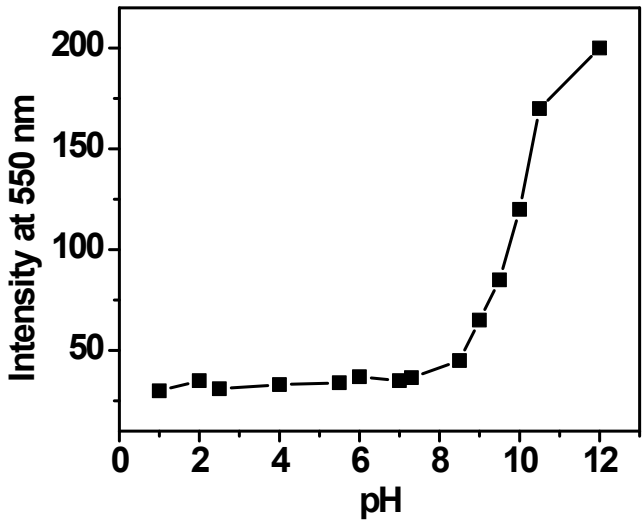

Figure S8: Fluorescence response of BPQ at 550 nm (10 μM) as a function of pH in CH_3CN/ H_2O (2/3, *v/v*), pH is adjusted by using aqueous solutions of 1 M HCl or 1 M NaOH.

8. Computational method

Full geometry optimizations were carried out using the density functional theory (DFT) method at the B3LYP [1-3] level for the compounds. All elements except cadmium were assigned 6-31+G(d) basis set. The LANL2DZ basis set with effective core potential (ECP) set of Hay and Wadt [4] was used for Cd. The vibrational frequency calculations were performed to ensure that the optimized geometries represent the local minima and there were only positive eigen values. Vertical electronic excitations based on B3LYP optimized geometries were computed using the time-dependent density functional theory (TDDFT) formalism [5-7] in methanol using conductor-like polarizable continuum model (CPCM) [8-10]. All calculations were performed with Gaussian09 program package [11] with the aid of the GaussView visualization program.

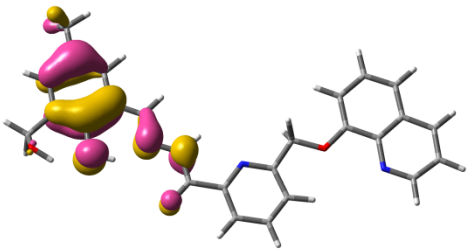

HOMO (E = -5.758 eV)

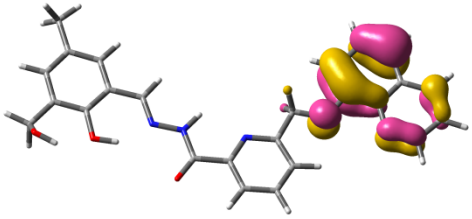

HOMO-1 (E = -6.038 eV)

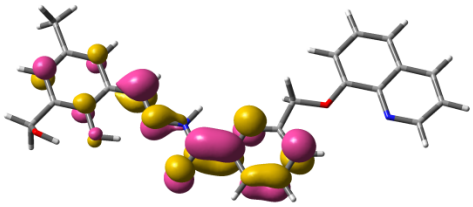

LUMO (E = -1.848 eV)

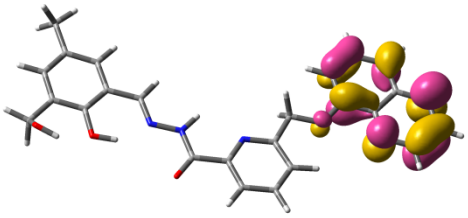

LUMO+1 (E = -1.492 eV)

Figure S9: Contour plot of selected molecular orbitals of BPQ

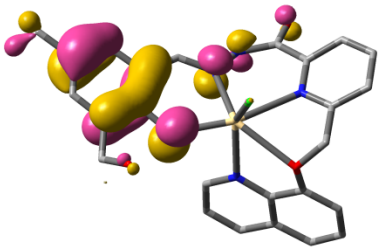

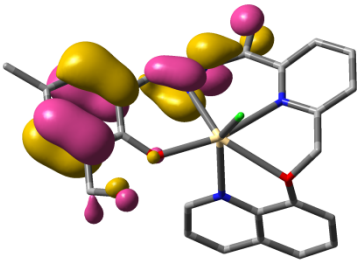

HOMO (E = -5.015 eV)

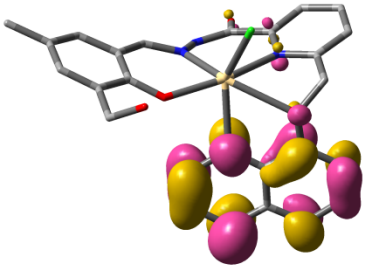

LUMO (E = -2.282 eV)

HOMO-1 (E = -6.072 eV)

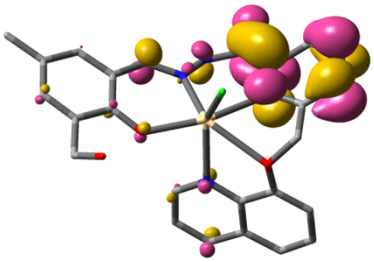

LUMO+1 (E = -2.129 eV)

Figure S10: Contour plot of selected molecular orbitals of BPQ-Cd^{2+}

Table S1. Vertical electronic excitations of BPQ and BPQ-Cd^{2+} calculated by TDDFT/B3LYP/CPCM method

Compound	Excitation	Excitation wavelength (nm)	Oscillator strength (au)	$\lambda_{expt.}$ (nm)
BPQ	HOMO→LUMO	357	0.3905	364
	HOMO-1→LUMO+1	311	0.1635	
	HOMO-2→LUMO	308	0.2640	
BPQ-Cd^{2+}	HOMO→LUMO	442	0.1184	460
	HOMO→LUMO+2	363	0.1021	
	HOMO-1→LUMO	328	0.1252	

9. Live-cell imaging:

Cell experiments were done using pretreated Cd^{2+} with the cells and pictures were acquired after screening several slides and performing the experiments in triplicate. The objective of this experiment is to show that even a minute quantity of Cd^{2+} can be efficiently detected by the probe. No one would expect that the live cells will have the probe, but it is possible that live cells will have Cd^{2+} due to environmental pollution or toxic chemicals. That is why the cells are first treated with Cd^{2+} to mimic the situation and probe is used to detect Cd^{2+} which penetrated into the cells. The nuclear stain DAPI helps to detect the Cd^{2+} treated cells under dark field where no other fluorescence was detected. But as the cells were treated with probe, Cd^{2+}-probe complex emitted bright green fluorescence as shown in Fig. 6b.

However here we have treated cells first with the BPQ and then Cd^{2+} was added to the cells. The pictures were given below.

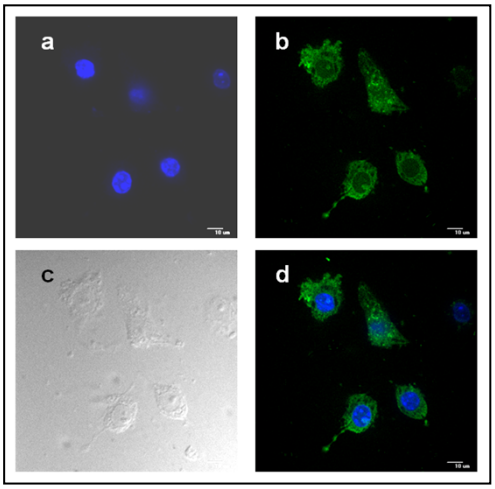

Figure S11: Confocal microscopic images of probe in RAW 264.7 cells pre-treated with BPQ: (a) BPQ treatment only at 1 μM concentration, nuclei counterstained with DAPI (1 μg/ml), (b) treatment a followed by $CdCl_2$ at concentration 20 μM, (c) bright field image of the cells after treatment (d) overlay image in dark field. All images were acquired with a 40× objective lens.

10. ^{1}H NMR spectrum of BPQ

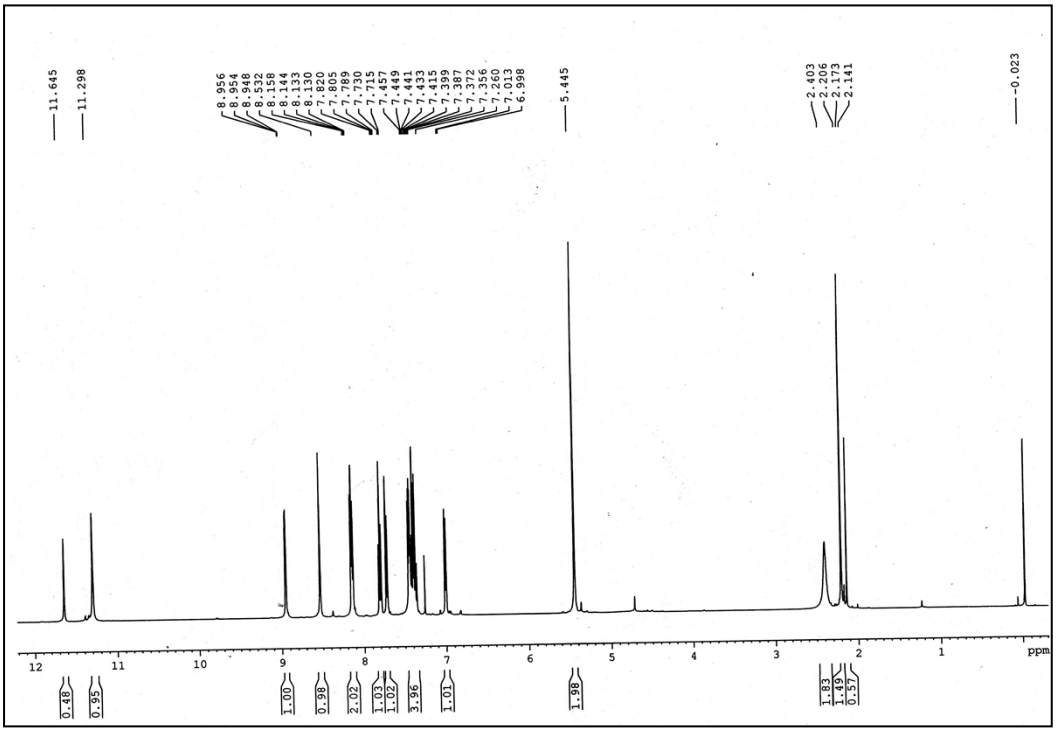

Figure S12: ^{1}H NMR (400 MHz) spectrum of BPQ in $CDCl_3$.

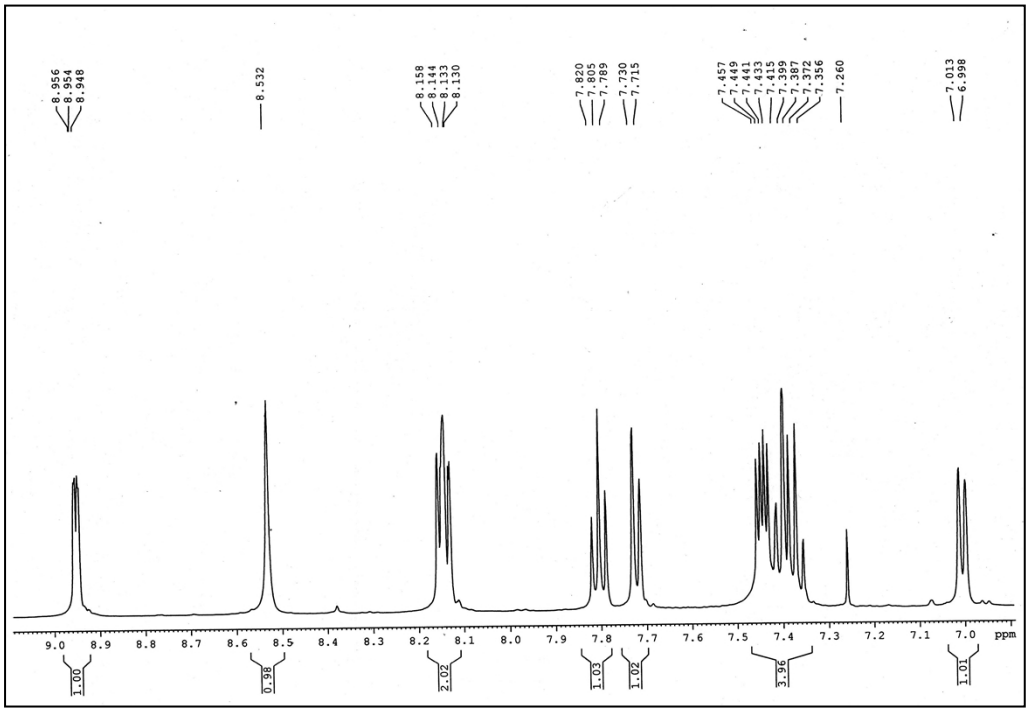

Figure S13: ^{1}H NMR (expansion) spectrum of BPQ.

11. ^{13}C NMR spectrum of BPQ

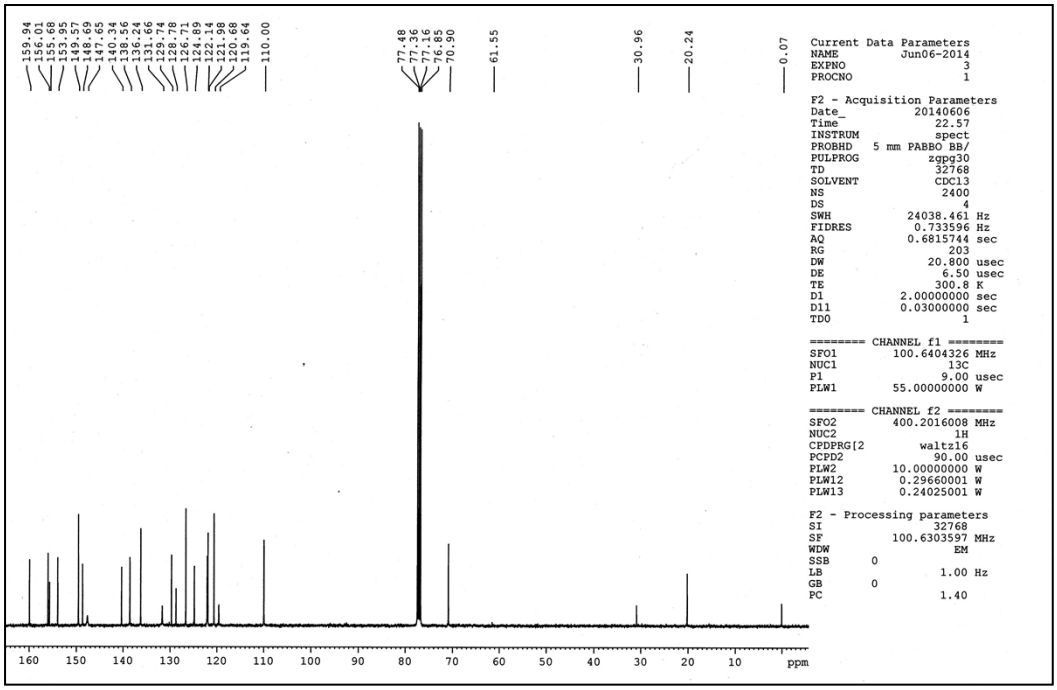

Figure S14: ^{13}C NMR (100 MHz) spectrum of BPQ in $CDCl_3$.

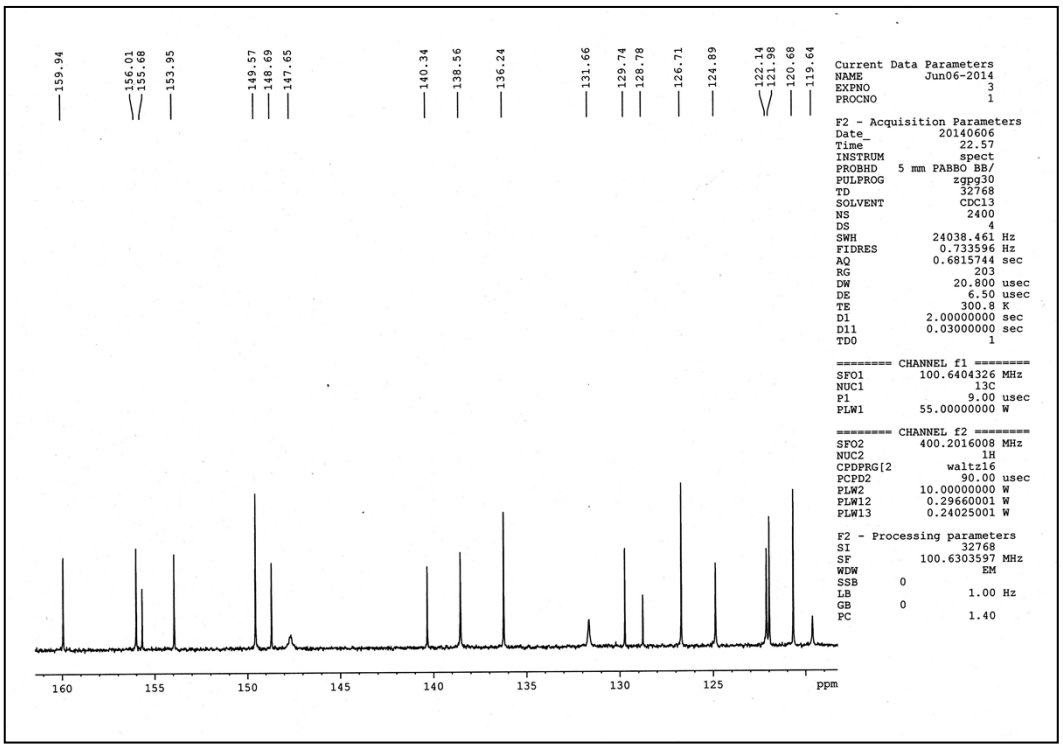

Figure S15: ^{13}C NMR (expansion) spectrum of BPQ.

12. Mass spectrum (HRMS) of BPQ

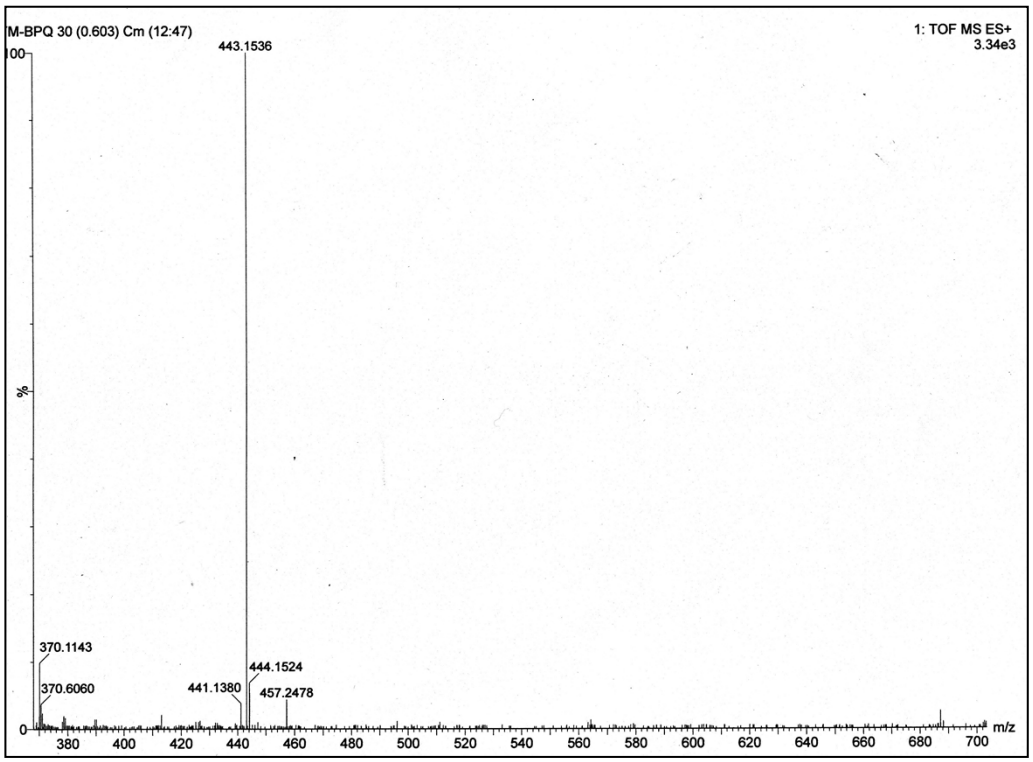

Figure S16: HRMS of BPQ.

13. ^{1}H NMR titration of BPQ with Cd^{2+}

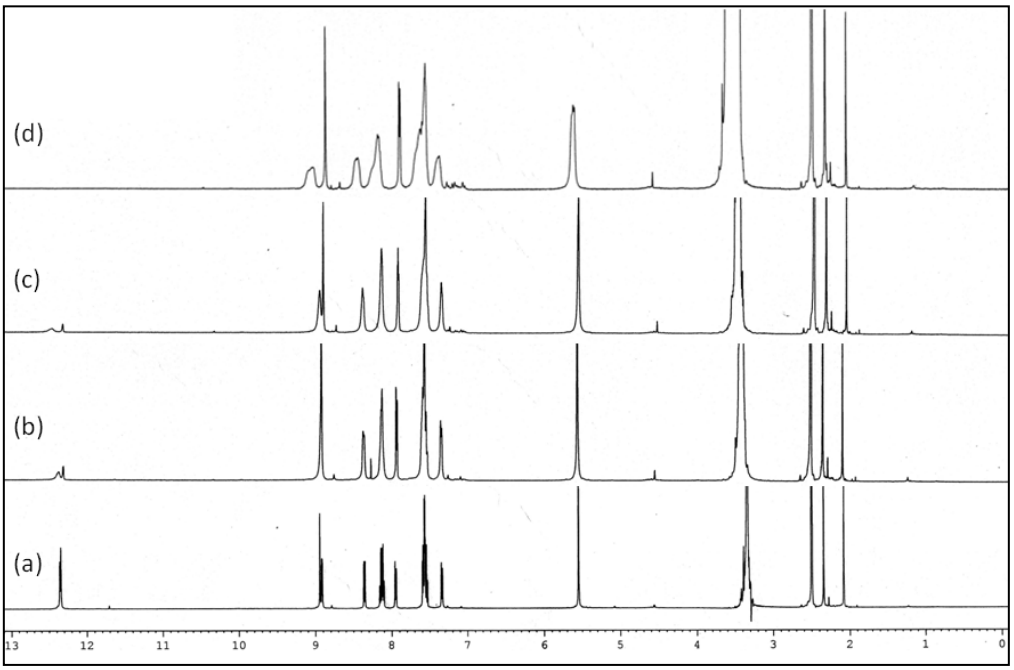

Figure S17: ^{1}H NMR (400 MHz) spectra of (a) BPQ (Conc. = 7.2×10^{-3} M), (b) [BPQ + $CdCl_2$ (3.6×10^{-3} M)], (c) [BPQ + $CdCl_2$ (7.2×10^{-3} M)] and (d) [BPQ + $CdCl_2$ (1.4×10^{-2} M)] in d^6 DMSO containing 1% D_2O.

14. IR spectra of BPQ and its Cd^{2+}complexes

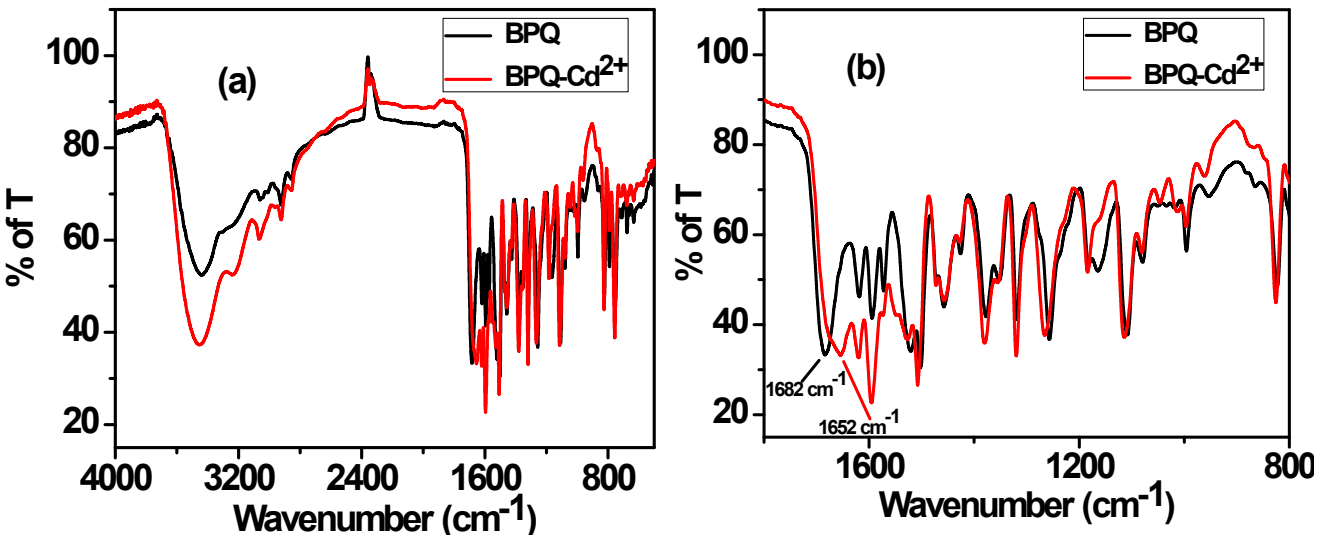

Figure S18: FT IR spectra of (a) BPQ and its complex with Cd^{2+} and (b) same in expansion mode.

14. ESI-MS spectrum of Cd^{2+} complex of BPQ

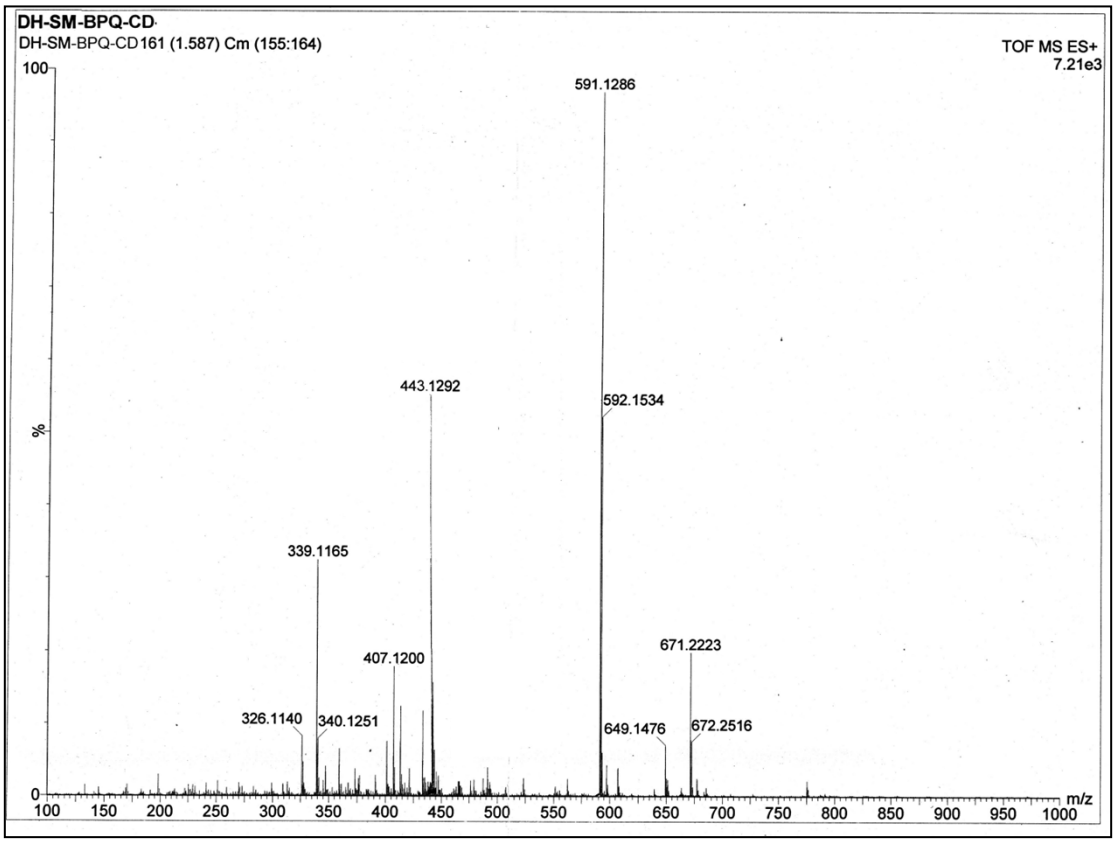

Figure S19: HRMS of BPQ+Cd^{2+}

14. References:

[1] A.D. Becke, J. Chem. Phys. 98 (1993) 5648–5652.

[2] C. Lee, W. Yang, R. G. Parr, Phys. Rev. B 37 (1988) 785–789.

[3] D. Andrae, U. Haeussermann, M. Dolg, H. Stoll and H. Preuss, Theor. Chim. Acta 77 (1990) 123–141.

[4] P. J. Hay, W. R. Wadt, J. Chem. Phys. 82 (1985) 299.

[5] R. Bauernschmitt, R. Ahlrichs, Chem. Phys. Lett. 256 (1996) 454–464.

[6] R.E. Stratmann, G.E. Scuseria, M.J. Frisch, J. Chem. Phys. 109 (1998) 8218–8224.

[7] M.E. Casida, C. Jamorski, K.C. Casida, D.R. Salahub, J. Chem. Phys. 108 (1998) 4439–4449.

[8] V. Barone, M. Cossi, J. Phys. Chem. A 102 (1998) 1995–2001.

[9] M. Cossi, V. Barone, J. Chem. Phys. 115 (2001) 4708–4717.

[10] M. Cossi, N. Rega, G. Scalmani, V. Barone, J. Comput. Chem. 24 (2003) 669–681.

[11] Gaussian 09, Revision D.01, M. J. Frisch, G. W. Trucks, H. B. Schlegel, G. E. Scuseria, M. A. Robb, J. R. Cheeseman, G. Scalmani, V. Barone, B. Mennucci, G. A. Petersson, H. Nakatsuji, M. Caricato, X. Li, H. P. Hratchian, A. F. Izmaylov, J. Bloino, G. Zheng, J. L. Sonnenberg, M. Hada, M. Ehara, K. Toyota, R. Fukuda, J. Hasegawa, M. Ishida, T. Nakajima, Y. Honda, O. Kitao, H. Nakai, T. Vreven, J. A. Montgomery, Jr., J. E. Peralta, F. Ogliaro, M. Bearpark, J. J. Heyd, E. Brothers, K. N. Kudin, V. N. Staroverov, R. Kobayashi, J. Normand, K. Raghavachari, A. Rendell, J. C. Burant, S. S. Iyengar, J. Tomasi, M. Cossi, N. Rega, J. M. Millam, M. Klene, J. E. Knox, J. B. Cross, V. Bakken, C. Adamo, J. Jaramillo, R. Gomperts, R. E. Stratmann, O. Yazyev, A. J. Austin, R. Cammi, C. Pomelli, J. W. Ochterski, R. L. Martin, K. Morokuma, V. G. Zakrzewski, G. A. Voth, P. Salvador, J. J. Dannenberg, S. Dapprich, A. D. Daniels, Ö. Farkas, J. B. Foresman, J. V. Ortiz, J. Cioslowski, and D. J. Fox, Gaussian, Inc., Wallingford CT, 2009.